

Effects of Tower Shadowing on Anemometer Data

William David Lubitz¹

¹Assistant Professor, School of Engineering, University of Guelph, Guelph, ON, Canada,
wlubitz@uoguelph.ca

ABSTRACT

The tower supporting an anemometer modifies the local wind field and the measurements of the anemometer. The impact on wind speed is most pronounced within the tower wake, however, the entire local flow field is impacted. In fields such as wind energy resource assessment, where anemometer data must be as accurate as possible, tower-induced flow modification contributes a non-negligible amount of uncertainty to the wind resource assessment. A model to remove these “tower shadow” effects from anemometer data is proposed that uses a potential flow solution in the region outside the tower wake, and a Gaussian turbulent wake within the wake. The input data required for the model has been intentionally limited to data typically available for wind resource assessment purposes. When applied to anemometer data collected for wind resource assessment purposes from two different towers, the model predicts reasonable correction factors for the raw anemometer data. An attempt is made to reduce prediction error further by adding an averaging period correction that requires only mean and standard deviation wind direction data. An initial comparison of model predictions to measured data suggests that additional factors need to be considered if more accurate corrections are to be generated. Initial results suggest the model may be a useful tool for first-order correction of anemometer data, however the model is not able to remove significant variability in the anemometer data that may be due to higher order effects or different phenomena, and additional model validation is needed.

INTRODUCTION

Tower-mounted anemometers are the standard method of collecting wind data for wind energy resource assessments. Locating an anemometer on the top of the tower is ideal since there are no wind directions that result in the anemometer having tower structure upwind, and flow distortion is below 2% [1]. However, this configuration is often not possible. If anemometers are needed at heights other than the tower top, or more than one sensor must be placed at the tower top, an anemometer will be mounted on the end of a horizontal boom extending horizontally outwards from the tower. The anemometer must be properly positioned at the end of the boom, so that it projects upwards high enough to avoid flow distortions caused by the boom. The effect of the boom on the flow field can become significant if the anemometer is less than 15 boom diameters above the boom [1].

The presence of the tower induces a local wind field different from the ambient flow. Field and wind tunnel measurements have confirmed the common characteristics of the flow field around a meteorological tower [3-9]. Directly upwind of the tower, wind speeds are reduced relative to ambient. Laterally local wind speeds are increased. Continuing around the tower toward the downwind side, wind speed continues to increase until the edge of the tower wake is approached. Within the region $\pm 30^\circ$ of the downwind direction is the tower wake region with greatly reduced wind speeds and increased turbulence.

To avoid measurement errors due to these flow distortions, the anemometer should be located as far from the tower horizontally as practical. NREL suggested minimum distances of three and six tower diameters for lattice and tubular towers respectively [9]. IEC 16400-12-1

Appendix G [1] includes formulae to estimate the velocity deficit experienced by an anemometer as a function of distance upwind from a boom, and suggest that a distance of 5.7 times tower width will keep velocity deficit to less than 0.5% for a lattice tower of 0.5 porosity. Overall, a minimum distance of 7 tower widths is considered to be conservative [11]. Note that in practice, boom length is limited by increasing boom size (which can also cause interference) and the need to maintain rigidity.

In all of the above-cited publications, measurements within the tower wake region are excluded from consideration, since departures of mean velocity and turbulence from ambient within the wake are an order of magnitude greater than perturbations of the flow in other regions around the tower. Common practice is to not use anemometer data from wind directions that put the anemometer in the tower wake. However, cases where the wake region is unavoidable do arise. Sensor failures or the use of available data collected for other purposes may allow investigation using only a single anemometer. For small wind turbines, wind resource assessments and performance verifications are often constrained to a single anemometer. Placing two boom-mounted anemometers at the same level on different sides of a tower keeps at least one anemometer out of the wake region for all wind directions, however measurements from both anemometers must still be assimilated in a consistent manner.

A model that can remove the tower-induced flow distortion from anemometer measurements due to the tower would give a truer representation of the wind climate at a site. The goal of this study is the development of a practical model to correct anemometer measurements for tower-induced flow perturbations. A key goal is for the model to be implementable in spreadsheet or wind analysis software.

FLOW FIELD AROUND A TOWER

Towers for meteorological or wind energy measurements are typically of two types: tubular towers, in which a single vertical circular tube is supported by one or more sets of guy wires, and lattice towers, in which three or four vertical members are connected by a network of smaller cross-members. The latter type may be guyed or freestanding. Anemometer booms have also been affixed to more massive pre-existing structures (e.g.[5]), however these installations will not be considered here.

Tubular towers consist of a single round tube supported by guy wires. Depending on the height of the tower, the tube diameter is typically in the range of 5 – 25 cm. The wind field around the tower can be approximated as the flow around a two dimensional cylinder. Limiting consideration to wind speeds greater than the typical wind turbine cut-in speed of 4 m/s, Reynolds number based on tube diameter is greater than 10,000, and while the flow around the tube will be laminar, the far wake behind the tube will be turbulent [12]. Flow around the tube begins transitioning from laminar to turbulent at a Reynolds number of approximately 3×10^5 , which results in delayed separation and a narrower wake region. For a 25 cm diameter tower, this represents a wind speed of only 8 m/s, and therefore this phenomenon will be expected to have an impact for wind resource assessment purposes.

Lattice towers consist of many discrete elements each generating a discrete wake, however, outside of a near field region the flow field can be approximated as the wake of a single bluff body. Measurements at a lattice mast at the Brookhaven National Laboratory (USA) observed the velocity deficit in the tower wake had a Gaussian cross-section at anemometers spaced less than one tower width from the tower [7]. Both velocity deficit in the wake, and speed-up lateral to the tower, were independent of wind speed and slightly dependent on Richardson number.

WAKE PROPERTIES

Flow around a two dimensional bluff body is one of the most studied problems in fluid mechanics. The width of a two-dimensional turbulent plane wake varies as the square root of distance downwind of wake origin [13]. This means that specifying wake properties as a function of wind direction angle (where width varies linearly with distance downwind) will be conservative as the distance downwind increases.

Wucknitz [14] found a potential flow model could predict the wind speed error of a boom-mounted anemometer, but noted that Reynolds number dependency should exist even in this case. Wucknitz subsequently refined his model with an adjustment for the size of the wake, which is Reynolds number dependent [14]. A similar approach, using a laminar flow predicted wind field to correct wind speeds measured by anemometers, was employed at a large diameter tower in Hungary, although in this case multiple anemometers were available [5]. Computational fluid dynamics has also been applied using an actuator disk approach [3,11]. The potential approach has the advantage of being easier to implement for new anemometer installations, and both methods give results for flow distortion outside the wake region that are in overall agreement with each other and measurements. While it is possible to use more complex methods such as large eddy simulation for specific situations, more intensive approaches are unlikely to result in a significantly useful improvement in accuracy, especially if the goal is to be able to apply results to different anemometer installations.

One area that has not been investigated is the effect of averaging time on wind speeds measured in wakes. Dabberdt [7] calculated the measured mean velocity deficit as a function of wind direction, and then applied that data as a correction factor in an attempt to remove the effect of being in the tower wake from anemometer measurements. A small improvement was noted, although large uncertainty remained. It is likely that the use of hourly average wind speeds, with no accounting for variation in wind direction at shorter timescales, and consequently variability of the anemometer position within the wake over the averaging period, is a significant contributor to this remaining uncertainty. However, to the knowledge of the authors, the effect of averaging period on wake shadow corrections does not appear to have been reported in the literature. Since wind resource assessments are typically based on 10 minute or hourly average wind speeds, this area requires investigation.

MODEL

This section details the formulation of a model to predict the velocity defect measured at a boom-mounted anemometer a horizontal distance r from the center of the tower. It is assumed the tower can be represented by a characteristic diameter or width d , with shape and smaller features accounted for by a drag coefficient C_d . Anemometers must be in the far-wake region ($r > 3d$), and at a height well below the top of the tower so that the impact of tower end effects on the flow field are negligible. The impact of tower guy wires is assumed negligible. Ambient wind speed U_∞ is restricted to be greater than 4 m/s. The velocity defect u is the difference between U_∞ and the local wind speed U . (i.e., $u = U_\infty - U$), which will be determined by superimposing the effects of a turbulent wake and a potential flow.

WAKE MODEL

The wake region downwind of the tower is modeled as a Gaussian two-dimensional turbulent wake behind a bluff body, with momentum deficit constant in the downwind direction x and

centerline velocity deficit decaying as $x^{-1/2}$. From Schlichting [12], the centerline velocity defect in a turbulent wake taken to be

$$u_{CL} = 1.15U_{\infty} \left(\frac{C_d d}{x} \right)^{1/2} \quad (1)$$

where x is the distance downwind from the tower along the wake centerline. The drag D on a two-dimensional object is $D = \frac{1}{2}C_d \rho d U_{\infty}^2$, and the drag is also $D = \rho U_{\infty} q$ where ρ is air density and q is the momentum deficit. Combining these two relations gives $q = \frac{1}{2}C_d U_{\infty} d$. Momentum deficit has been assumed constant at any distance downwind so that for any positive x ,

$$q = \int_{-\infty}^{\infty} u dy = \frac{1}{2} C_d U_{\infty} d \quad (2)$$

At any distance x downwind, it will also be assumed the wake has a Gaussian profile of the form

$$u_w = \frac{A}{s\sqrt{2\pi}} \exp\left(-\frac{y^2}{2s^2}\right) \quad (3)$$

where u_w is the velocity defect in the wake, y is the lateral distance from the wake centerline, and A and s are parameters that will now be determined based on the constraints of equations 1 and 2. At the centerline, $y = 0$ and $u_w = u_{CL}$, and from equations 1 and 3,

$$u_{CL} = \frac{A}{s\sqrt{2\pi}} \quad (4)$$

The value of the integral of equation (3) with respect to y from ∞ to $-\infty$ is equal to A . Doing this and equating the result with equation (2) gives

$$A = \frac{1}{2} C_d U_{\infty} d \quad (5)$$

Substituting this into equation 4 and equating with equation 1 gives

$$s = 0.173\sqrt{C_d dx} \quad (6)$$

The result is an analytical wake model that can be used to calculate velocity defect at any point x and y using the combination of equations 3, 5 and 6, given d and C_d of the tower and U_{∞} .

POTENTIAL MODEL

The flow distortion in the non-wake region is modeled using a potential flow in a similar manner to Wucknitz [12]. The reduced mass flow in the wake region is simulated by adding a source of

strength m_1 at the tower, and sink of strength m_2 a short distance a downstream in the positive x direction. The velocity potential ϕ at a given point is

$$\frac{\phi}{U_\infty} = x + m_1 \ln\left(\sqrt{x^2 + y^2}\right) - m_2 \ln\left(\sqrt{(x-a)^2 + y^2}\right) \quad (7)$$

and the resulting velocity defect due to potential flow u_p at a given point (x,y) is

$$u_p = U_\infty - \nabla \phi \quad (8)$$

Setting the value of m_1 greater than m_2 simulates the introduction of extra mass flow by the source and sink combination, displacing the non-wake region of the potential flow field in a similar manner as if it was displaced by a turbulent wake. Note however, that close to the source and sink (within the near-wake region) the velocities predicted by the potential flow model are not representative of a real wake.

The values a , m_1 and m_2 are parameters that must be determined. These were varied iteratively until values were found that were consistent with the survey of field measurements reported by Wucknitz [12]. The values $a = d$, $m_1 = 0.53C_d d$, and $m_2 = 0.27C_d d$ were used in the results presented here.

COMBINED MODEL

The final predicted velocity at a point (x,y) is found by combining the velocity defects predicted by both models, and noting that the wake model is only valid for $x > 0$:

$$U = \begin{cases} U_\infty - u_w - u_p & x > 0 \\ U_\infty - u_p & x \leq 0 \end{cases} \quad (9)$$

Note that because the potential model velocity deficits are not physically realistic near the sink, the restriction that the model is not valid in the near wake ($r > 3d$) is important. Within the wake, u_w is much greater than u_p , and while it is not physically correct to add the effect of u_p in this region, doing so produces an automatic transition between wake and potential models at the wake boundary that would otherwise have to be defined and implemented.

RESULTS

The model was used to produce correction factors for two cases representing the most common tower arrangements in utility-scale wind energy resource assessment. Data was obtained for a communication tower at Red Oak, Iowa, USA, and an NRG tilt-up mast at Algona, Iowa, USA (Table 1). Both towers have two anemometers at 50 m, and booms on the east and west sides.

Figure 1 shows the velocity field predicted by the model for the Red Oak tower for $U_\infty = 10$ m/s. The circle shows $r/d = 3$, both the anemometer distance and near-wake limit of the model. Note that the contour interval varies: it is 0.1 m/s between 9 and 11 m/s, and 1.0 m/s otherwise. The source at (0,0) and sink (1,0), as well as the extreme values of the local flow field around them, are both clearly visible. In the far wake region, the flow field is Gaussian, shows reduced wind speeds directly upwind, and accelerated flow along the sides of the tower, with greater effect downwind.

Figures 2 and 3 show the ratio of anemometer velocities at each of towers overlaid with the ratios predicted by the model. Velocity ratios are much greater for the lattice tower (Red Oak) than for the tilt-up tower (Algona), which is expected given the smaller diameter of a tubular tilt-up tower. Tower wake effects are clearly visible at both towers. The model underestimates wake width at the communication tower. The structure is complex with $r/d \approx 3$, at the limit of model applicability. It has been observed that a Gaussian wake velocity distribution appears rapidly downwind of a lattice tower [e.g. 7], and the measurements here are consistent with that observation.

Table 1. Tower data

Parameter	Red Oak	Algona
Tower type	Lattice	Monopole tilt-up
Data	1995 – 1999	1996
d	1.0 m	0.2 m
C_d	0.6	1.2
r/d	3	7.5

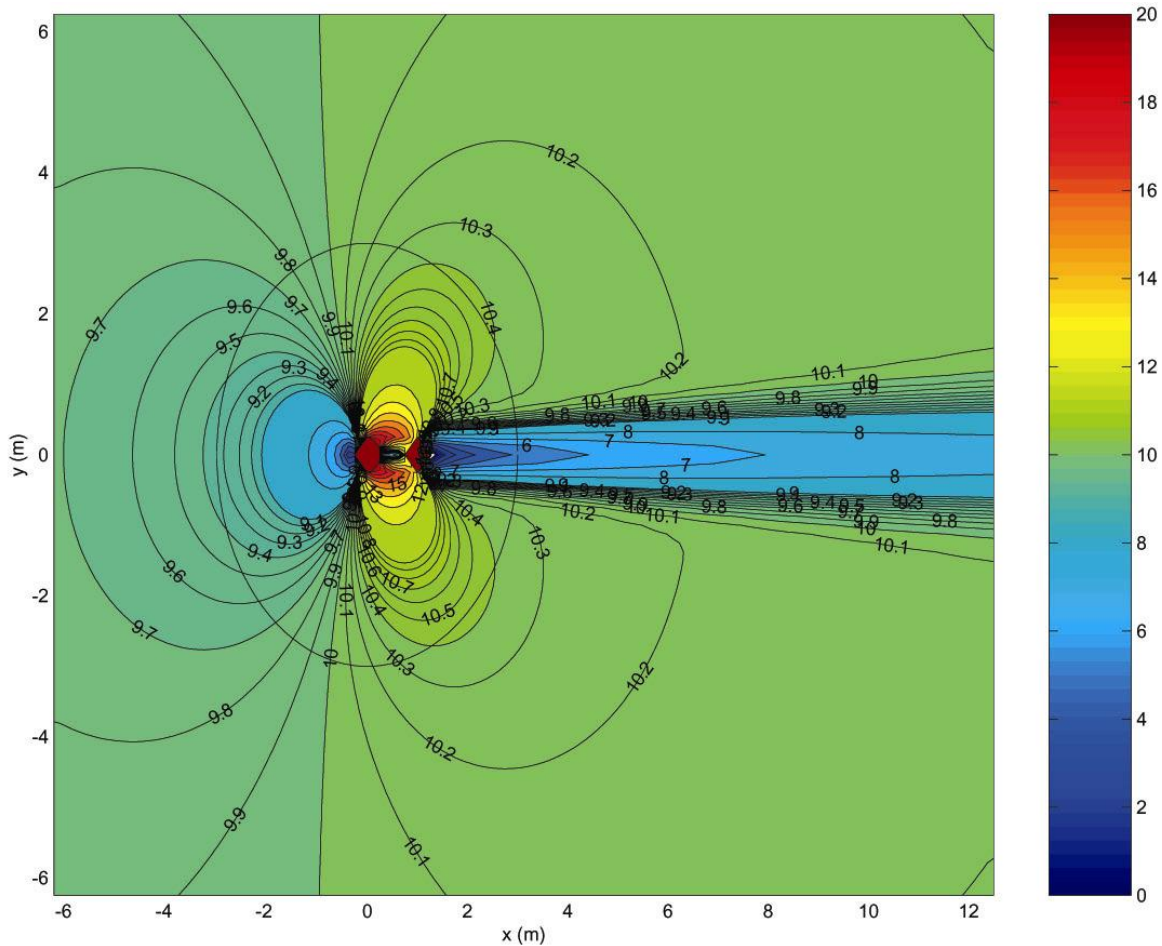


Figure 1. Wind field predicted for 10 m/s ambient wind at Red Oak tower.

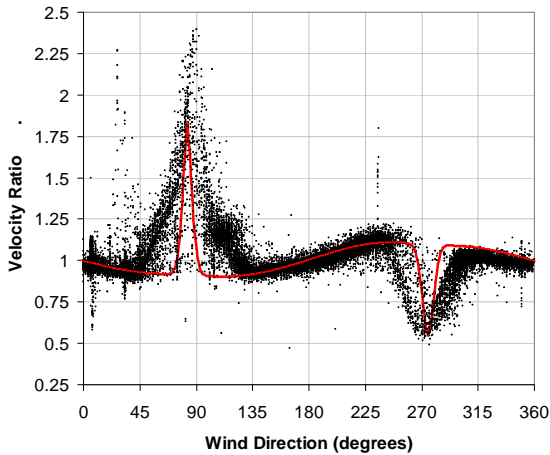


Figure 2. Red Oak communication tower velocity ratios.

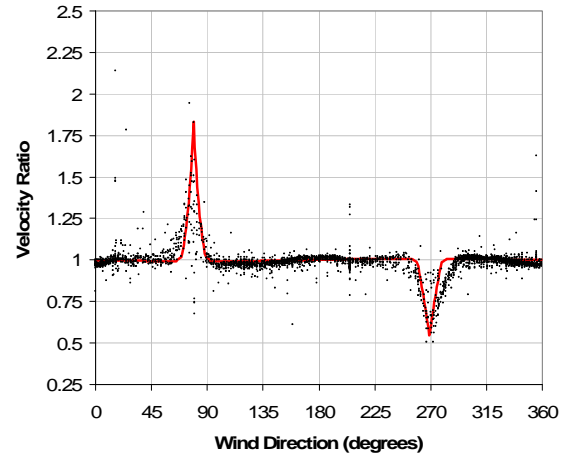


Figure 3. Algona tilt-up tower velocity ratios.

At both towers, there is considerable spread in the velocity ratios when one anemometer is partially or completely in the tower wake, with measured velocity ratios often less than predicted by the model. At the same time, the wind direction range over which the wake has an impact is under-predicted by the model in both cases, substantially so for Red Oak.

Non-wake velocity variations are apparent, and reasonably well-matched by the model in figure 2. Owing to the greater distance of the anemometers from the tower in figure 3, these variations are difficult to discern in figure 3. The maximum non-wake velocity ratios predicted for the tilt-up tower are about 1%, which is within the noise level of the data. For the tilt-up tower, the wake correction is the main contribution that can be provided by the model.

AVERAGING PERIOD CORRECTION

Measurements for wind energy resource assessment typically use a one to three second sample rate, but a 10 minute (or somewhat less commonly, one hour) averaging period is used to reduce demands on datalogger storage and simplify post-processing. Often, for each 10 minute or hourly observation, only the mean and standard deviations of the values are recorded.

In both of the case studies above, the predicted wake region was narrower, with greater velocity deficit, than was measured at the towers. It was hypothesized that the use of hourly average wind speeds, with no accounting for variation in wind direction at shorter timescales, and consequently variability of the anemometer position within the wake over the averaging period, was a significant contributor to this variation in velocity ratio. A method of correcting the tower shadow model in the previous section to include these effects was desired. Modeling of the impact of averaging period on wake shadow corrections does not appear to have been reported in the literature.

Often, the only available measurement of wind direction variability within the averaging period of a wind observation is the wind direction standard deviation. The mean wind directions recorded during the previous, and next, observations could also be utilized. This is a small amount of additional data with which to reconstruct the temporal variation in wind direction within the averaging period.

Two approaches for estimating the distribution of wind direction within an observation are considered. The first method (“Method A”) generates a wind direction distribution for an observation by fitting a Gaussian distribution to the mean wind direction and standard deviation of the observation. The resulting probability distribution function p is

$$p(\theta)_{i,A} = \frac{1}{\sigma_i \sqrt{2\pi}} \exp\left(-\frac{(\theta_i - \theta_{avg,i})^2}{2\sigma_i^2}\right) \quad (10)$$

where θ is the wind direction, and $\theta_{avg,i}$ and σ_i are the average wind direction and standard deviation of the wind direction for observation i . The predicted ratio of the anemometer wind speeds for observation i would then be

$$R_{i,A} = \int p(\theta)_{i,A} R(\theta) d\theta \quad (11)$$

where $R(\theta)$ is the anemometer velocity ratio as a function of wind direction predicted by the method derived in the prior section.

This approach requires assuming that the wind direction within the observation is Gaussian distributed. While Gaussian distributions do occur in wind related phenomena (and were used in the wake model previously derived), the wind direction will usually not be Gaussian distributed because the wind direction signal is a composite of short time scale (less than the averaging period) variations due to gusts and turbulence, and longer time scale variations due to weather. However, given the data available, it is felt that the Gaussian distribution is the best available.

The longer time scale variations are accounted for by a second method (“Method B”). Fourth order polynomial curves are fit to the components of the unit vector of the mean wind direction values of five consecutive observations, with the observation of interest being the middle observation (e.g. $\theta_{avg,i-2}$, $\theta_{avg,i-1}$, $\theta_{avg,i}$, $\theta_{avg,i+1}$, $\theta_{avg,i+2}$). The two vector component curve fits are then converted back to angles, giving a single continuous function of wind direction versus time (i.e., $\theta_{avg,i}(t)$). This prediction of wind direction as a function of time is then sampled within the averaging period to give a wind direction probability distribution function for the observation (i.e., $p(\theta)_{i,B}$). The values of $R(\theta)$ are then integrated with the probability distribution function in the same manner as Method A (equation 11).

Finally, Method C combines both approaches, assuming that wind direction varies with time based on mean wind direction observations, and that at any instant in time the wind direction is Gaussian distributed, instead of being simply a single direction value. It is assumed in all of the methods that the flowfield is quasi-stationary and that the steady state model previously derived adequately describes the flow field at any given instant in time.

As an initial test, each averaging time correction method was applied to the predicted anemometer velocity ratios at the Red Oak and Algona towers. Prediction error of each method was quantified using mean error (ME) and mean absolute errors (MAE):

$$ME = \frac{1}{n} \sum_{i=1}^n R_{i,pred} - R_{i,meas} \quad (12)$$

$$MAE = \frac{1}{n} \sum_{i=1}^n |R_{i,pred} - R_{i,meas}| \quad (13)$$

where $R_{i,pred}$ and $R_{i,meas}$ are the predicted and measured anemometer velocity ratio for the i 'th observation. Table 2 gives ME and MAE at each tower, for the base case of no averaging time correction, and for each of the three methods outlined above.

Table 2. Anemometer velocity ratio prediction errors for averaging period correction methods.

	Red Oak		Algona	
	ME	MAE	ME	MAE
No averaging correction	0.0018	0.071	-0.019	0.033
Method A (Gaussian)	0.0030	0.069	-0.018	0.029
Method B (Curve Fit)	0.0013	0.070	-0.019	0.032
Method C (Gaussian + Curve Fit)	0.0026	0.069	-0.018	0.030

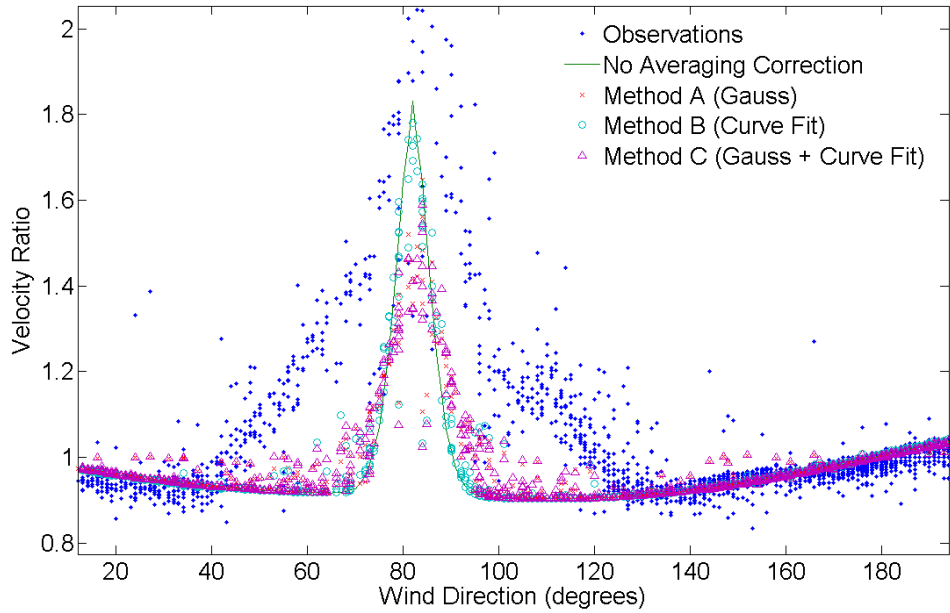


Figure 4. Example of averaging period correction applied to Red Oak.

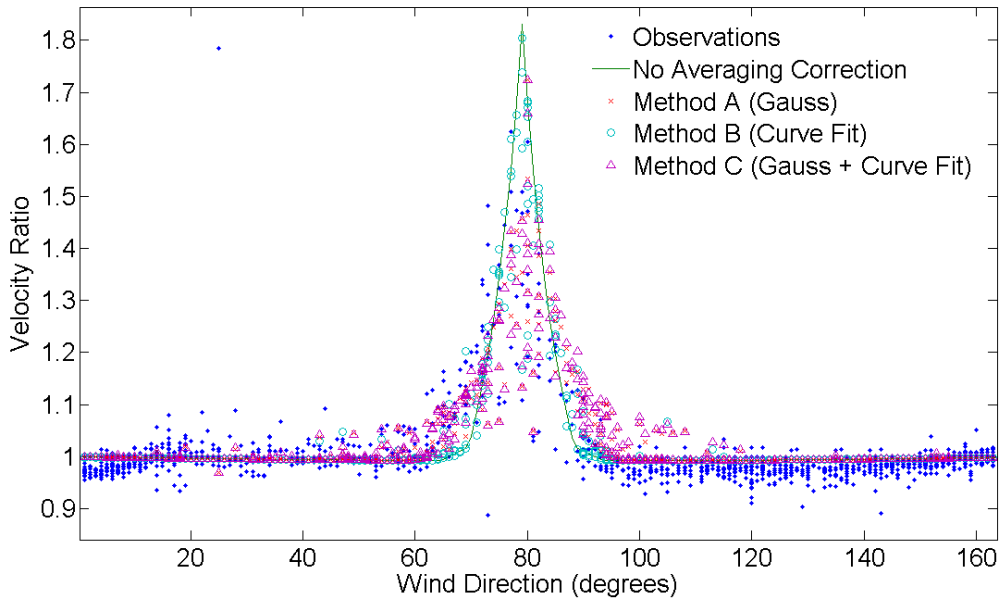


Figure 5. Averaging-period correction methods applied to Algona

Overall, the effects of the averaging period correction schemes on prediction accuracy appear to be minor. Figures 4 and 5 show representative examples of the corrected predictions for each method at Red Oak and Algona. (In both cases, only a subset of wind directions are shown, and for Red Oak, only 12% of available data has been plotted to retain clarity in the plot.) Qualitatively, the methods produce a distribution of predicted ratios that is a better match to the measured data than the predictions from the base case model. Velocity deficits predicted by the methods within the wake are lower, but the directions over which the wake is apparent increase.

For the directions not influenced by the wake, the variation of the measured ratios is still greater than the variation of the predicted values, even for Method C. Since the majority of observations are in these regions (the anemometer booms on the towers were located so as not to be aligned with prevailing wind directions), the noise related to these observations reduces the apparent effect of observations within the wake when *ME* and *MAE* are calculated. Overall, it appears that while the model may be able to make a first order correction for gross effects of tower-induced flow, much of the variation in the measured velocity ratios is noise that the model cannot resolve. There are many possible sources of this noise beyond the tower shadowing effects examined here, including temperature or icing effects, atmospheric stability, electrical noise, anemometer wear or contamination, cup overspeed, and the influence of smaller tower elements such as guy wires, booms or mounting brackets. Some of these effects could potentially be incorporated into the model, however, additional measurement parameters would likely be required. If the model remains constrained to using only mean and standard deviations of wind speed and direction, it appears that it will be difficult to achieve significantly improved correction accuracy.

CONCLUSION

A preliminary model for correcting anemometer readings to remove tower-induced wind field perturbations has been developed. The model only requires data that would be readily available from a typical wind resource assessment anemometer installation: basic tower parameters, mean wind speed, and the mean and standard deviation of the wind direction. This simplicity also poses inherent limits on the model: initial testing with data from two anemometer towers suggests that significant noise in the data is not removed or explained by the model. Additional testing and verification is needed before the model is used in practice.

Methods of correcting for wind direction variance at timescales less than the data averaging period, based on measurements typically taken for wind resource assessment, were examined. These methods appeared to produce an improvement in prediction accuracy when examined qualitatively, however, mean error and mean absolute error values calculated for the two towers show only a very small quantitative improvement over the base case of using the model without an averaging period correction.

The results of the two case studies examined support the recommendation by prior investigators that mounting anemometers on booms greater than 7 tower diameters should limit tower flow distortion effects to a lower magnitude than the sensor uncertainty of the anemometer itself. For anemometers on long booms, the main value of the model would be the wake correction.

ACKNOWLEDGEMENT

Keith Kutz of the Iowa Energy Center generously provided access to wind data used in this study.

REFERENCES

- [1] Perrin, D., McMahon, N., Crane, M., Ruskin, H., Crane, L., Hurley, B. *The Effect of a Meteorological Tower on Its Top-Mounted Anemometer. Applied Energy.* (84) 413-424. 2007.
- [2] IEC 61400-12-1. *Wind Turbines – Part 12-1: Power Performance Measurements of Electricity Producing Wind Turbines. Edition 1.0. IEC. Dec. 2005.*
- [3] Pedersen, B. M., Hansen, K. S., Øye, S., Brinch, M., Fabian, O. *Some Experimental Investigations on the Influence of the Mounting Arrangements on the Accuracy of Cup-Anemometer Measurements. J. Wind Eng. & Ind. Aero.* (39) 373-383. 1992.
- [4] Barthlott, C., Fielder, F. *Turbulence Structure in the Wake Region of a Meteorological Tower. Boundary-Layer Meteorology.* (108) 175-190. 2003.
- [5] Bartholy, J., Radics, K. *Wind Profile Analyses and Atmospheric Stability Over a Complex Terrain in Southwestern Part of Hungary. Physics and Chemistry of the Earth.* (30) 195-200. 2005.
- [6] Cermak, J. E., Horn, J. D. *Tower Shadow Effects. Journal of Geophysical Research.* v. 73 iss. 6, 1869-1876. 1968.
- [7] Dabberdt, W. F. *Tower-Induced Errors in Wind Profile Measurements. J. App. Met.* 7, 359-366. June, 1968.
- [8] Izumi, Y., Barad, M. L. *Wind Speeds as Measured by Cup and Sonic Anemometers and Influenced by Tower Structure. J. App. Met.* (9) 851-856. Dec. 1970.
- [9] Wucknitz, J. *Disturbance of Wind Profile Measurements By A Slim Mast. Boundary-Layer Meteorology.* (11) 155-169. 1977.
- [10] Bailey, B. H., McDonald, S. L. *Wind Resource Assessment Handbook. National Renewable Energy Laboratory. April 1997.*
- [11] Hansen, M. O. L., Pedersen, B. M. *Influence of the Meteorology Mast on a Cup Anemometer. J. Solar Energy Engineering.* 121 (2), 128-131. 1999.
- [12] Simiu, E., Scanlan, R. H. *Wind Effects on Structures. John Wiley & Sons. 1978.*
- [13] Schlichting, H., Gersten, K. *Boundary-Layer Theory. 8th Ed. Springer, 2000.*
- [14] Wucknitz, J. *Flow Distortion by Supporting Structures. In: Air-Sea Interactions. Dobson, F., Hasse, L., Davis, R. eds. Plenum Press. New York. 1980.*